Journal of Applied and Numerical Analysis
2025, Vol. 3, pp. 18–27
doi: 10.30970/ana.2025.3.18

On the comparison of the boundary integral equations method and the method of fundamental solutions for a 3D boundary value problem for the Helmholtz equation

Ihor Borachok[1], Svyatoslav Lavryk[1]

[1] *Faculty of Applied Mathematics and Informatics, Ivan Franko National University of Lviv, 1, Universytets'ka str., 79000, Lviv, Ukraine*

Анотація. Розглядається порівняльне дослідження методу граничних інтегральних рівнянь (ГІР) та методу фундаментальних розв'язків (МФР) для чисельного розв'язування внутрішньої задачі Діріхле для тривимірного рівняння Гельмгольца з комплексним хвильовим числом. Метод ГІР базується на поданні розв'язку у вигляді потенціалу подвійного шару та передбачає розв'язування інтегрального рівняння Фредгольма другого роду із використанням квадратур на поверхнях, дифеоморфних до одиничної сфери. МФР апроксимує розв'язок лінійною комбінацією фундаментальних розв'язків із точками джерела, розміщеними за межами області, а невідомі коефіцієнти визначаються за допомогою колокації на межі області. Чисельні експерименти проведено для областей з аналітичною параметризацією з використанням точних розв'язків для перевірки похибок. Результати демонструють, що МФР часто забезпечує кращу точність, проте має місце погана обумовленість матриці системи, на відміну від більш стійкої системи методу ГІР. Дослідження висвітлює компроміси між точністю, стійкістю та обчислювальною складністю, властиві обом методам.

Abstract. This article presents a comparative study of the Boundary Integral Equations Method (BIEM) and the Method of Fundamental Solutions (MFS) for the numerical solution of the interior Dirichlet problem for the 3D Helmholtz equation with complex wave number. The BIEM approach is based on the representation of the solution via a double-layer potential and involves solving a Fredholm integral equation of the second kind using quadrature rules on surfaces diffeomorphic to the sphere. The MFS approximates the solution using a linear combination of fundamental solutions with source points placed outside the domain and determines the unknown coefficients by collocation on the boundary. Numerical experiments are conducted on geometries with analytic parametrizations, using exact solutions for error validation. The results demonstrate that while MFS often achieves higher accuracy, it suffers from severe ill-conditioning, unlike the more stable BIEM system. The study highlights the trade-offs in accuracy, stability, and computational complexity inherent to both methods.

Key words: Helmholtz equation, Dirichlet problem, boundary integral equations method, Nyström method, Wienert quadratures, method of fundamental solutions.

1 Introduction

Helmholtz-type equations have many different applications, for example, in problems of heat conductivity, structural vibrations, wave scattering, and fluid-solid interaction, see [17]. Since problems for the Helmholtz equation are widely used, there are a large number of methods for their numerical solution. Popular numerical methods are the finite element method [16], the finite difference method [25], BIEM [18], and meshless methods [23]. For the most part, the case of two-dimensional problems is more studied, but there are also many studies of various problems for the Helmholtz equation in three-dimensional domains. In this article, we continue the study of three-dimensional problems for the Helmholtz equation, focusing on two main approaches: BIEM and MFS, and compare their effectiveness.

The BIEM is often used to solve boundary value problems, see [8,18]. It has been successfully used to numerically solve three-dimensional problems for the Laplace equation, based on the representation of the solution in the form of a single layer potential [7]. Taking into account the boundary data, a system of boundary integral equations is obtained, which is discretized by the Galerkin method in a combination with Gauss-Legendre type quadrature rules, proposed by Wienert [24]. A similar algorithm is used for the numerical solution of boundary value problems for the Helmholtz equation in [13, 15]. In addition, in the mentioned works it is shown that under the condition of sufficient smoothness of the input data and the boundary of the domain, the superalgebraic order of convergence can be guaranteed. In [20] the Nyström method based on the Wienert's [24] trigonometric product-rectangle quadratures has been used. In our work, we use the representation of the solution in the form of a double layer potential and use the Nyström method based on Gauss-Legendre type quadratures to numerically solve the integral equation of the second kind.

The MFS is a popular meshless technique for solving various boundary value problems. It was first introduced by Kupradze and Aleksidze in [19], and later applied to elliptic problems in [6, 9, 12]. It is also widely used for the numerical solution of boundary value problems for the Helmholtz equation in 2D and 3D domains in [5, 21]. In MFS, the unknown function is approximated by a linear combination of the fundamental solutions, with source points placed outside the solution domain. By applying the collocation method, a system of linear equations is obtained to find the unknown coefficients. The method exhibits high approximation accuracy, is simple to implement, and requires relatively few computations.

Let us formulate the problem to be studied more precisely. Let $D \subset \mathbb{R}^3$ be a bounded simply connected domain with a sufficiently smooth boundary Γ. The goal is to find a function $u \in C^2(D) \cap C(\overline{D})$ such that it satisfies the Helmholtz equation with a complex-valued parameter

$$\Delta u(\boldsymbol{x}) + \kappa^2 u(\boldsymbol{x}) = 0, \quad \boldsymbol{x} \in D, \ \kappa \in \mathbb{C}, \ \mathrm{Im}(\kappa) > 0 \tag{1.1}$$

and the Dirichlet boundary condition

$$u(\boldsymbol{x}) = f(\boldsymbol{x}), \quad \boldsymbol{x} \in \Gamma. \tag{1.2}$$

For the Helmholtz equation with a complex parameter $\kappa \in \mathbb{C}$ and positive imaginary part $\mathrm{Im}(\kappa) > 0$, it is known that under suitable assumptions on the boundary Γ and for sufficiently smooth boundary data f, the solution of the Dirichlet problem exists and is unique, see [11, 14] and the references therein.

The structure of the article is as follows. In Sections 2 and 3, we apply the BIEM and MFS, respectively, for the numerical solution of the problem (1.1)-(1.2). The results of numerical experiments for both approaches are presented in Section 4, while the final conclusions are summarized in Section 5.

2 Boundary Integral Equations Method

In this section, we apply BIEM to numerically solve the problem (1.1)-(1.2). The solution of the problem can be written in the form of a double layer potential

$$u(\boldsymbol{x}) = \int\limits_{\Gamma} \varphi(\boldsymbol{y}) \frac{\partial \Phi(\boldsymbol{x}, \boldsymbol{y})}{\partial \nu(\boldsymbol{y})} ds(\boldsymbol{y}), \quad \boldsymbol{x} \in D, \tag{2.1}$$

where $\varphi \in C(\Gamma)$ is the unknown potential density, ν is the unit outward normal vector to Γ and Φ is a fundamental solution of the Helmholtz equation

$$\Phi(\boldsymbol{x}, \boldsymbol{y}) = \frac{1}{4\pi} \frac{e^{i\kappa|\boldsymbol{x}-\boldsymbol{y}|}}{|\boldsymbol{x}-\boldsymbol{y}|}, \quad \boldsymbol{x}, \boldsymbol{y} \in \mathbb{R}^3, \ \boldsymbol{x} \neq \boldsymbol{y}. \tag{2.2}$$

Applying the jump relations of the double-layer potential at the boundary [18], the function (2.1) is a solution of the problem (1.1)-(1.2) if the density φ is a solution of the Fredholm integral equation of the second kind

$$-\frac{1}{2}\varphi(\boldsymbol{x}) + \int\limits_{\Gamma} \varphi(\boldsymbol{y}) \frac{\partial \Phi(\boldsymbol{x}, \boldsymbol{y})}{\partial \nu(\boldsymbol{y})} ds(\boldsymbol{y}) = f(\boldsymbol{x}), \quad \boldsymbol{x} \in \Gamma. \tag{2.3}$$

We assume that the boundary Γ is diffeomorphic to the unit sphere $\mathbb{S}^2$

$$\mathbb{S}^2 = \{p(\theta, \phi) = (\sin\theta\cos\phi, \sin\theta\sin\phi, \cos\theta), \ (\theta, \phi) \in [0, \pi] \times [0, 2\pi)\}.$$

Then there exists an analytic mapping $q : \mathbb{S}^2 \to \Gamma$ with a given non-zero Jacobian J, describing the surface Γ.

Performing a change of variables in equation (2.3), we obtain the parametrized integral equation on $\mathbb{S}^2$

$$-\frac{1}{2}\psi(\hat{\boldsymbol{x}}) + \int\limits_{\mathbb{S}^2} \psi(\hat{\boldsymbol{y}}) \, K(\hat{\boldsymbol{x}}, \hat{\boldsymbol{y}}) \, ds(\hat{\boldsymbol{y}}) = \tilde{f}(\hat{\boldsymbol{x}}), \quad \hat{\boldsymbol{x}} \in \mathbb{S}^2, \tag{2.4}$$

where, for simplicity, we denoted

$$\psi(\hat{\boldsymbol{x}}) = \varphi(q(\hat{\boldsymbol{x}})), \quad \tilde{f}(\hat{\boldsymbol{x}}) = f(q(\hat{\boldsymbol{x}})), \quad \hat{\boldsymbol{x}} \in \mathbb{S}^2,$$

$$K(\hat{\boldsymbol{x}}, \hat{\boldsymbol{y}}) = \frac{\partial \Phi(q(\hat{\boldsymbol{x}}), q(\hat{\boldsymbol{y}}))}{\partial \nu(q(\hat{\boldsymbol{y}}))} J(\hat{\boldsymbol{y}}), \quad \hat{\boldsymbol{x}}, \hat{\boldsymbol{y}} \in \mathbb{S}^2, \ \hat{\boldsymbol{x}} \neq \hat{\boldsymbol{y}}.$$

Note, $K(\hat{\boldsymbol{x}}, \hat{\boldsymbol{y}})$ is a weakly singular integral kernel that can be written in the form

$$K(\hat{\boldsymbol{x}}, \hat{\boldsymbol{y}}) = \frac{M(\hat{\boldsymbol{x}}, \hat{\boldsymbol{y}})}{|\hat{\boldsymbol{x}} - \hat{\boldsymbol{y}}|}, \quad \hat{\boldsymbol{x}}, \hat{\boldsymbol{y}} \in \mathbb{S}^2, \ \hat{\boldsymbol{x}} \neq \hat{\boldsymbol{y}}$$

with

$$M(\hat{\boldsymbol{x}}, \hat{\boldsymbol{y}}) = \frac{e^{i\kappa|q(\hat{\boldsymbol{x}}) - q(\hat{\boldsymbol{y}})|}}{4\pi} \frac{(q(\hat{\boldsymbol{y}}) - q(\hat{\boldsymbol{x}}), \, \nu(q(\hat{\boldsymbol{y}})))}{|q(\hat{\boldsymbol{x}}) - q(\hat{\boldsymbol{y}})|^2} \frac{|\hat{\boldsymbol{x}} - \hat{\boldsymbol{y}}| J(\hat{\boldsymbol{y}})}{|q(\hat{\boldsymbol{x}}) - q(\hat{\boldsymbol{y}})|} \left(i\kappa|q(\hat{\boldsymbol{x}}) - q(\hat{\boldsymbol{y}})| + 1\right).$$

Theorem 2.1. *For any $f \in C(\Gamma)$ equation (2.3) has a unique solution φ in $C(\Gamma)$.*

Proof. We present a sketch of proof. Due to the weak singularity of $K(\hat{\boldsymbol{x}}, \hat{\boldsymbol{y}})$, operator in the left-hand side of (2.3) is compact by the Theorem 2.6 in [11]. For the homogeneous right-hand side $f = 0$, taking into account that interior Dirichlet problem has at most one solution (see theorem

(3.10) in [11]), it implies $\varphi = 0$. By the Riesz theory [18][Ch. 3, Thm. 3.4 and Cor. 3.5] the boundary integral equation (2.3) has a unique solution for any $f \in C(\Gamma)$. □

Note, due to the analyticality of q well-posedness of (2.3) also applies to (2.4). In order to discretize (2.4), we consider Gauss-Legendre quadrature rules, proposed by Wienert [24].

For a given space discretization parameter $N \in \mathbb{N}$ the following values are defined

$$\hat{\boldsymbol{p}}_{\beta,\mu} = p\left(\vartheta_\beta, \varphi_\mu\right), \vartheta_\beta = \arccos \xi_\beta,\ \varphi_\mu = \frac{\pi}{N}\mu,$$

$$w_\beta^{(1)} = \frac{2\pi}{N(1-\xi_\beta^2)\left(P_N'(\xi_\beta)\right)^2}, \quad \beta = 1, \ldots, N,\ \mu = 0, \ldots, 2N-1,$$

where $\xi_1 < \cdots < \xi_N$ are the zeros of the Legendre polynomials P_N [1].
For a given function $f \in C(\mathbb{S}^2 \setminus \{(0,0,\pm 1)\})$ approximation A_N is defined as

$$(A_N f)(\hat{\boldsymbol{x}}) = \sum_{\beta=1}^{N} \sum_{\mu=0}^{2N-1} w_\beta^{(1)} f(\hat{\boldsymbol{p}}_{\beta,\mu})\ a_{\beta,\mu}(\hat{\boldsymbol{x}}), \tag{2.5}$$

where $a_{\beta,\mu}(\hat{\boldsymbol{x}}) = \sum_{n=0}^{N-1} \frac{2n+1}{4\pi} P_n(\hat{\boldsymbol{x}} \cdot \hat{\boldsymbol{p}}_{\beta,\mu})$ and by $\hat{\boldsymbol{x}} \cdot \hat{\boldsymbol{p}}_{\beta,\mu}$ we denote a scalar product of two vectors.
Note, the poles are excluded from the continuity requirements, since values of the parametrized functions $f \circ p$ at the poles may depend on the direction of approach (i.e. specific value of ϕ) and may be not continous at the poles.
For the non-singular integrands, the following quadrature rule can be used

$$\int_{\mathbb{S}^2} f(\hat{\boldsymbol{y}})\, ds(\hat{\boldsymbol{y}}) \approx \int_{\mathbb{S}^2} (A_N f)(\hat{\boldsymbol{y}})\, ds(\hat{\boldsymbol{y}}) = \sum_{\beta=1}^{N} \sum_{\mu=0}^{2N-1} w_\beta^{(1)} f(\hat{\boldsymbol{p}}_{\beta,\mu}). \tag{2.6}$$

For the weakly singular integrands, the following quadrature rule can be used

$$\int_{\mathbb{S}^2} \frac{f(\hat{\boldsymbol{y}})}{|\hat{\boldsymbol{n}}_p - \hat{\boldsymbol{y}}|}\, ds(\hat{\boldsymbol{y}}) \approx \int_{\mathbb{S}^2} \frac{(A_N f)(\hat{\boldsymbol{y}})}{|\hat{\boldsymbol{n}}_p - \hat{\boldsymbol{y}}|}\, ds(\hat{\boldsymbol{y}}) = \sum_{\beta=1}^{N} \sum_{\mu=0}^{2N-1} w_\beta^{(2)} f(\hat{\boldsymbol{p}}_{\beta,\mu}), \tag{2.7}$$

where $w_\beta^{(2)} = w_\beta^{(1)} \sum_{n=0}^{N-1} P_n(\xi_\beta)$ and $\hat{\boldsymbol{n}}_p = (0,0,1)$.

Both quadratures are obtained by approximation of the regular part of the integrand via approximation A_N and then using exact integration. According to results in [24], these quadrature rules have super-algebraic or even exponential convergence order, depending on the smoothness of f.

By simple substitution, the quadrature rule (2.7) can be extended to a more general case

$$\int_{\mathbb{S}^2} \frac{f(\hat{\boldsymbol{y}})}{|\hat{\boldsymbol{x}} - \hat{\boldsymbol{y}}|}\, ds(\hat{\boldsymbol{y}}) = \int_{\mathbb{S}^2} \frac{f(T_{\hat{\boldsymbol{x}}}^{-1}\hat{\boldsymbol{y}})}{|\hat{\boldsymbol{n}}_p - \hat{\boldsymbol{y}}|}\, ds(\hat{\boldsymbol{y}}) \approx \sum_{\beta=1}^{N} \sum_{\mu=0}^{2N-1} w_\beta^{(2)} f(T_{\hat{\boldsymbol{x}}}^{-1}\hat{\boldsymbol{p}}_{\beta,\mu}),\ \hat{\boldsymbol{x}} \in \mathbb{S}^2, \tag{2.8}$$

where $T_{\hat{\boldsymbol{x}}}$ is usually a rotation, such that $T_{\hat{\boldsymbol{x}}}\hat{\boldsymbol{x}} = \hat{\boldsymbol{n}}_p$, see [24].

Applying (2.8) to the integral in (2.4), we get an approximation equation

$$-\frac{1}{2}\psi(\hat{\boldsymbol{x}}) + \sum_{\beta=1}^{N} \sum_{\mu=0}^{2N-1} w_\beta^{(2)} \psi(T_{\hat{\boldsymbol{x}}}^{-1}\hat{\boldsymbol{p}}_{\beta,\mu})\, M(\hat{\boldsymbol{x}}, T_{\hat{\boldsymbol{x}}}^{-1}\hat{\boldsymbol{p}}_{\beta,\mu}) = \tilde{f}(\hat{\boldsymbol{x}}), \quad \hat{\boldsymbol{x}} \in \mathbb{S}^2. \tag{2.9}$$

We observe that (2.9) contains values of the density ψ in the rotated nodes $T_{\hat{\boldsymbol{x}}}^{-1}\hat{\boldsymbol{p}}_{\beta,\mu}$. In order to be able to construct a system of linear equations, we replace $\psi(T_{\hat{\boldsymbol{x}}}^{-1}\hat{\boldsymbol{p}}_{\beta,\mu})$ with its approximation by A_N (2.5)

$$\psi(T_{\hat{\boldsymbol{x}}}^{-1}\hat{\boldsymbol{p}}_{\beta,\mu}) \approx (A_N\psi)(T_{\hat{\boldsymbol{x}}}^{-1}\hat{\boldsymbol{p}}_{\beta,\mu}) = \sum_{\beta'=1}^{N}\sum_{\mu'=0}^{2N-1} w_{\beta'}^{(1)}\psi(\hat{\boldsymbol{p}}_{\beta',\mu'})a_{\beta',\mu'}(T_{\hat{\boldsymbol{x}}}^{-1}\hat{\boldsymbol{p}}_{\beta,\mu}). \tag{2.10}$$

Substituting (2.10) back into (2.9), we get

$$-\frac{1}{2}\psi(\hat{\boldsymbol{x}}) + \sum_{\beta'=1}^{N}\sum_{\mu'=0}^{2N-1}\psi(\hat{\boldsymbol{p}}_{\beta',\mu'})w_{\beta',\mu'}^{(3)}(\hat{\boldsymbol{x}}) = \tilde{f}(\hat{\boldsymbol{x}}), \quad \hat{\boldsymbol{x}} \in \mathbb{S}^2, \tag{2.11}$$

where $w_{\beta',\mu'}^{(3)}(\hat{\boldsymbol{x}}) = w_{\beta'}^{(1)}\sum_{\beta=1}^{N}\sum_{\mu=0}^{2N-1} w_{\beta}^{(2)}\, M(\hat{\boldsymbol{x}}, T_{\hat{\boldsymbol{x}}}^{-1}\hat{\boldsymbol{p}}_{\beta,\mu})a_{\beta',\mu'}(T_{\hat{\boldsymbol{x}}}^{-1}\hat{\boldsymbol{p}}_{\beta,\mu})$.

Collocating the equation (2.11) in the nodes $\hat{\boldsymbol{p}}_{\beta_2,\mu_2},\ \beta_2 = 1,\dots,N,\ \mu_2 = 0,\dots,2N-1$, we get a $2N^2 \times 2N^2$ system of linear equations for the unknown values $\psi(\hat{\boldsymbol{p}}_{\beta_2,\mu_2})$

$$-\frac{1}{2}\psi(\hat{\boldsymbol{p}}_{\beta_2,\mu_2}) + \sum_{\beta'=1}^{N}\sum_{\mu'=0}^{2N-1}\psi(\hat{\boldsymbol{p}}_{\beta',\mu'})w_{\beta',\mu'}^{(3)}(\hat{\boldsymbol{p}}_{\beta_2,\mu_2}) = \tilde{f}(\hat{\boldsymbol{p}}_{\beta_2,\mu_2}). \tag{2.12}$$

After solving (2.12), the approximate solution of (1.1)–(1.2) can be found by applying qudrature rule (2.6) to (2.1)

$$u_N(\boldsymbol{x}) = \sum_{\beta_2=1}^{N}\sum_{\mu_2=0}^{2N-1} w_{\beta_2}^{(1)}\psi(\hat{\boldsymbol{p}}_{\beta_2,\mu_2})\frac{\partial\Phi}{\partial\nu(\boldsymbol{y})}(\boldsymbol{x}, q(\hat{\boldsymbol{p}}_{\beta_2,\mu_2}))J(\hat{\boldsymbol{p}}_{\beta_2,\mu_2}), \quad \boldsymbol{x} \in D.$$

Although the system (2.12) defines a Nyström discretisation for the boundary integral equation, and error estimates for the quadrature rules are provided by Wienert in [24], the derivation of a rigorous error estimate for the $u_N(\boldsymbol{x})$ is not available. As discussed in [24] (Chapter 8), the quadrature weights $w_{\beta',\mu'}^{(3)}(\hat{\boldsymbol{x}})$ involve a rotation of the spherical grid such that each evaluation point $\hat{\boldsymbol{x}}$ is mapped to the north pole $\hat{\boldsymbol{n}}_p$. This procedure introduces a discontinuity near the south pole, since the rotation cannot be defined continuously over the entire sphere. As a result, the corresponding discrete integral operators no longer map into $C(\Gamma)$, which prevents the direct application of standard collectively compact operators convergence theory.

3 Method of fundamental solutions

In this section, we apply the MFS for the numerical solution of the problem (1.1)-(1.2). The function u is approximated by the linear combination of the narrowing of the fundamental solution (2.2)

$$u(\boldsymbol{x}) \approx \sum_{j=1}^{n}\alpha_j\Phi(\boldsymbol{x}, \boldsymbol{y}_j), \quad \boldsymbol{x} \in D, \tag{3.1}$$

where $n \in \mathbb{N}$, $\boldsymbol{y}_j \notin \overline{D}$, $j = 1,\dots,n$ are selected source points (or singularities) and $\alpha_j \in \mathbb{R}$, $j = 1,\dots,n$ are coefficients to be determined. Since the source points $\boldsymbol{y}_j$ are located outside the domain $\overline{D}$, the approximation (3.1) is well-defined for all $\boldsymbol{x} \in D$. In [3], it is shown that the basis $\{\Phi(\cdot, \boldsymbol{y}_j),\ j = 1,\dots,n\}$ is linearly independent and dense in $L_2(D)$.

The unknown coefficients are determined by collocating on the boundary Γ. As in the BIEM approach, we assume that there exists a describing function q for the boundary Γ. Then, the

collocation points $\boldsymbol{x}_k$, $k = 1, \ldots, m$, $m \in \mathbb{N}$ are uniformly distributed on the boundary Γ according to the following rule

$$\{\boldsymbol{x}_k\} = \{q(p(\theta_s, \phi_\rho))\}, \text{ with } \theta_s = \frac{\pi}{m'+1}s,\ s = 1, \ldots, m',\ \phi_\rho = \frac{\pi}{m'}\rho,\ \rho = 1, \ldots, 2m',$$

for $m' \in \mathbb{N}$, we then have a total of $m = 2(m')^2$ collocation points. Source points are uniformly distributed on an enlarged artificial surface by the following rule

$$\{\boldsymbol{y}_j\} = \left\{\eta q(p(\theta_{s'}, \phi_{\rho'}))\right\}, \text{ with } \theta_{s'} = \frac{\pi}{n'+1}s',\ s' = 1, \ldots, n',\ \phi_{\rho'} = \frac{\pi}{n'}\rho',\ \rho' = 1, \ldots, 2n',$$

where $\eta > 1$ is a magnification parameter and $n' \in \mathbb{N}$, having in total $n = 2(n')^2$ source points. Source points should be placed not too close and not too far from the boundary Γ. When the source points are located too close to the boundary, then the source and collocation points are close to each other, and this leads to singular behavior in the approximation. As the distance between the domain boundary and the source points increases, the results improve. However, placing the source points too far from the boundary results in an ill-conditioned matrix.

By imposing the boundary condition (1.2) at the collocation points, we obtain the following system of linear equations for finding the unknown coefficients

$$\sum_{j=1}^{n} \alpha_j \Phi(\boldsymbol{x}_k, \boldsymbol{y}_j) = f(\boldsymbol{x}_k), \quad k = 1, \ldots, m. \tag{3.2}$$

In general, the number of collocation points should be greater than or equal to the number of source points, $m \geq n$, see [10]. When $m > n$, the system (3.2) can be solved using the least squares method. In this research, we consider only boundaries diffeomorphic to the unit sphere, but it is obvious that the collocation and source points can be easily selected even in the case of more complex domain configurations. For more details about other distributions, we refer to [10].

MFS error estimation is less studied than for BIEM. Several studies have investigated the stability and convergence of the MFS for the 2D Helmholtz equation, as discussed in [4, 26]. Additionally, [4] notes that the MFS exhibits exponential convergence with respect to increasing n, for an admissible set of source points in circular domains and for analytical input data. The main drawback of the MFS is the high condition number of the matrix in the system (3.2). Sometimes, additional regularization techniques are required to obtain a stable solution, see, for example, [22]. It is also known that the condition number of the matrix is inversely proportional to the accuracy of the solution, see [2, 22].

4 Numerical examples

In this section we describe the results of two numerical experiments. For both examples, we use the exact analytical solution of the Helmholtz equation. To measure the accuracy of the numerical approximation, we use the following discrete L_2 error

$$E = \frac{1}{\tilde{N}} \left(\sum_{m=1}^{\tilde{N}} \sum_{j=1}^{\tilde{N}} |u_{ex}(\boldsymbol{x}_{m,j}) - u_{app}(\boldsymbol{x}_{m,j})|^2 \right)^{1/2}, \tag{4.1}$$

where u_{ex} is the exact solution, u_{app} is the approximate solution and $\tilde{N} = 10$. The test points $\boldsymbol{x}_{m,j}$ are uniformly distributed on a diminished artificial surface located within the solution domain D, according to the following rule

$$\boldsymbol{x}_{m,j} = 0.5q(p(\theta_m, \phi_j)),\ \theta_m = \frac{\pi}{\tilde{N}+1}m,\ \phi_j = \frac{2\pi}{\tilde{N}}j,\ \ m, j = 1, \ldots, \tilde{N}.$$

Example 4.1. In the first example, we consider the domain D (see Fig. 4.1a) with an acorn-type boundary surface Γ, with the following parametrization

$$\Gamma = \{r(\theta,\varphi)(\sin\theta\cos\phi, \sin\theta\sin\phi, \cos\theta),\ (\theta,\phi) \in [0,\pi]\times[0,2\pi]\}\,,$$

where $r(\theta,\varphi) = 0.2\left(0.6 + \sqrt{4.25 + 2\cos 3\theta}\right)$.

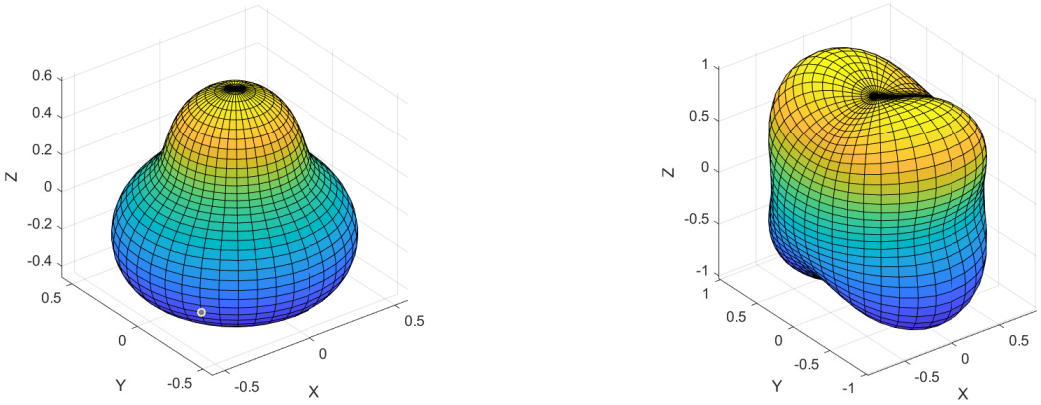

a) Domain in Example 4.1 b) Domain in Example 4.2

Fig. 4.1: Domains used in both examples.

As an exact solution, we use the narrowing of the fundamental solution (2.2)

$$u_{ex}(\boldsymbol{x}) = \Phi(\boldsymbol{x}, \boldsymbol{y}^*),\ \boldsymbol{x} \in D,\ \boldsymbol{y}^* = (0,0,5).$$

Then the boundary function is given as $f(\boldsymbol{x}) = \Phi(\boldsymbol{x}, \boldsymbol{y}^*)$, $\boldsymbol{x} \in \Gamma$. In both examples the magnification parameter used in MFS is $\eta = 2$. The value was chosen based on several numerical experiments, and is a good balance between good accuracy and an acceptable value of the matrix condition number.

Table 4.1 shows the errors E, computed by (4.1), for different values of κ and increasing N (or n), for both BIEM and MFS. Since for MFS the matrix becomes very ill-conditioned, Fig. 4.2 shows the dependence of errors and condition numbers of the final matrix, with increasing N (or n), for both BIEM and MFS, for $\kappa = 1$. As can be seen, for BIEM conditional number of the matrix remains the same and small, which contrasts with MFS, where the conditional number increases rapidly. However, on the other hand, the errors E in the case of using the MFS are smaller.

Table 4.1. Errors E, computed by (4.1), for different values of κ and increasing N (or n), for the Example 4.1.

BIEM					MFS				
N	Nodes	κ			n	m	κ		
		i	$1.1+1.3i$	$-1.3+1.9i$			i	$1.1+1.3i$	$-1.3+1.9i$
4	32	$3.60e-06$	$9.16e-07$	$6.21e-08$	32	72	$1.51e-07$	$5.58e-08$	$5.75e-09$
8	128	$3.31e-07$	$7.55e-08$	$4.52e-09$	128	200	$1.92e-09$	$7.89e-10$	$1.02e-10$
16	512	$1.38e-09$	$2.98e-10$	$2.28e-11$	288	392	$3.49e-11$	$1.61e-11$	$2.04e-12$
32	2048	$6.55e-12$	$7.95e-12$	$1.15e-12$	800	968	$1.00e-14$	$1.12e-14$	$1.56e-15$

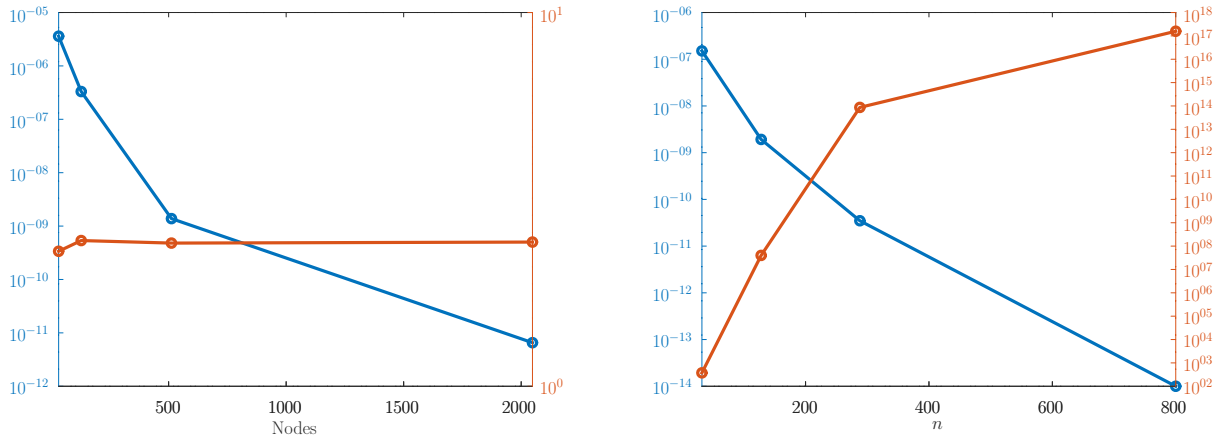

a) BIEM b) MFS

Fig. 4.2: Errors E (4.1) (blue color) and matrix condition numbers (red color), for both approaches, when $\kappa = i$ and N (or n) increases, in the Example 4.1.

Example 4.2. In the second example, we consider the domain D (see Fig. 4.1b) with a cushion-type boundary surface Γ, with the following parametrization

$$\Gamma = \{r(\theta,\varphi)(\sin\theta\cos\phi,\ \sin\theta\sin\phi,\ \cos\theta),\ (\theta,\phi) \in [0,\pi]\times[0,2\pi]\}\,,$$

where $r(\theta,\varphi) = \sqrt{0.8 + 0.2(\cos(2\varphi)-1)(\cos(4\theta)-1)}$.

As an exact solution, we use the following function

$$u_{ex}(\boldsymbol{x}) = e^{i\kappa x_1},\ \boldsymbol{x} \in D.$$

Then the boundary function is given as $f(\boldsymbol{x}) = e^{i\kappa x_1}$, $\boldsymbol{x} \in \Gamma$. Table 4.2 shows the errors E, calculated by (4.1), for different values of κ and increasing N (or n), for both BIEM and MFS.

Table 4.2. Errors E, computed by (4.1), for different values of κ and increasing N (or n), for the Example 4.2.

BIEM					MFS				
N	Nodes	κ			n	m	κ		
		i	$1.1+1.3i$	$-1.3+1.9i$			i	$1.1+1.3i$	$-1.3+1.9i$
4	32	$1.46e-02$	$1.23e-02$	$1.99e-02$	32	72	$3.67e-04$	$1.74e-03$	$3.58e-03$
8	128	$2.14e-03$	$2.14e-03$	$1.72e-03$	128	200	$2.57e-06$	$6.65e-06$	$1.18e-05$
16	512	$5.55e-05$	$3.74e-05$	$7.43e-05$	288	392	$3.88e-08$	$9.47e-08$	$1.30e-07$
32	2048	$4.73e-07$	$2.44e-06$	$6.16e-06$	800	968	$4.44e-09$	$3.94e-09$	$9.04e-09$

Numerical results are generated in Octave and executed on an ordinary workstation having an Intel(R) Core(TM) i7 CPU at 2.60 GHz. The typical computation time for BIEM for $N = 32$ is 300 seconds and for MFS for $n = 800$ is 60 seconds (time includes preparation of all results).

As the results of numerical experiments show, both methods provide good approximations for different domains D and input data f. In addition, both approaches are suitable for a wide range of parameter values κ. BIEM demonstrates higher stability: even with an increase in the discretization parameter N, the matrix condition number remains low. In contrast, MFS is distinguished by its simplicity of implementation and provides a more accurate approximation, but for large discretization parameters, it can lead to ill-conditioned matrices, which, in turn, can cause instability of the solution.

5 Conclusions

In this article, two effective approaches for the numerical solution of the three-dimensional interior Dirichlet problem for the Helmholtz equation with a complex wave number were investigated. MFS is characterized by simplicity of implementation, high speed and accuracy, while the BIEM, although more complex, demonstrates higher numerical stability. In future work, we plan to use both methods as components in the construction of more complex algorithms for solving non-stationary problems.

Declarations

Conflict of Interest.
The authors declare no conflict of interest.
Funding.
This research did not receive external funding.
Author Contributions.
All authors contributed equally to the research and preparation of this article.

References

1. Abramowitz, M., Stegun, I. A.: Handbook of Mathematical Functions with Formulas, Graphs, and Mathematical Tables. National Bureau of Standards Applied Mathematics Series, Washington, D. C. (1972)
2. Alves, C. J. S.: On the choice of source points in the method of fundamental solutions. Engineering Analysis with Boundary Elements. **33** (12), 1348-1361 (2009). doi:10.1016/j.enganabound.2009.05.007
3. Alves, C. J. S., Chen, C. S.: A new method of fundamental solutions applied to nonhomogeneous elliptic problems. Advances in Computational Mathematics. **23** (1), 125-142 (2005). doi:10.1007/s10444-004-1833-5
4. Barnett, A. H., Betcke, T.: Stability and convergence of the method of fundamental solutions for Helmholtz problems on analytic domains. Journal of Computational Physics. **227** (14), 7003-7026 (2008). doi:10.1016/j.jcp.2008.04.008
5. Bin-Mohsin, B., Lesnic, D.: The method of fundamental solutions for Helmholtz-type equations in composite materials. Computers & Mathematics with Application. **62** (12), 4377-4390 (2011). doi:10.1016/j.camwa.2011.10.006
6. Bogomolny, A.: Fundamental solutions method for elliptic boundary value problems. SIAM Journal on Numerical Analysis. **22** (4), 644-669 (1985). doi:10.1137/0722040
7. Borachok, I., Chapko, R., Johansson, B. T.: Numerical solution of a Cauchy problem for Laplace equation in 3-dimensional domains by integral equations. Inverse Problems in Science and Engineering. **24** (9), 1550-1568 (2016). doi:10.1080/17415977.2015.1130042
8. Chapko, R., Johansson, B. T.: On the numerical solution of a Cauchy problem for the Laplace equation via a direct integral equation approach. Inverse Problems and Imaging. **6** (1), 25-38 (2012). doi:10.3934/ipi.2012.6.25
9. Cheng, A. H. D., Hong, Y.: An overview of the method of fundamental solutions – Solvability, uniqueness, convergence, and stability. Engineering Analysis with Boundary Elements. **120**, 118-152 (2020). doi:10.1016/j.enganabound.2020.08.013
10. Chen, C. S., Karageorghis, A., Li, Y.: On choosing the location of the sources in the MFS. Numerical Algorithms. **72** (1), 107-130 (2016). doi:10.1007/s11075-015-0036-0
11. Colton, D., Kress, R.: Integral Equation Methods in Scattering Theory. John Wiley & Sons, New York (1983), XII + 271 pp.

12. Fairweather, G., Karageorghis, A.: The method of fundamental solutions for elliptic boundary value problems. Advances in Computational Mathematics. **9** (1), 69-95 (1998). doi:10.1023/A:1018981221740
13. Ganesh, M., Graham, I. G.: A high-order algorithm for obstacle scattering in three dimensions. Journal of Computational Physics. **198** (1), 211-242 (2004). doi:10.1016/j.jcp.2004.01.007
14. Graham, I. G., Pembery, O. R., Spence, E. A.: The Helmholtz equation in heterogeneous media: A priori bounds, well-posedness, and resonances. Journal of Differential Equations. **266** (6), 2869-2923 (2019). doi:10.1016/j.jde.2018.08.048
15. Graham, I., Sloan, I.: Fully discrete spectral boundary integral methods for Helmholtz problems on smooth closed surfaces in $\mathbb{R}^3$. Numerische Mathematik. **92**, 289-323 (2002). doi:10.1007/s002110100343
16. Ihlenburg, F., Babuška, I.: Finite element solution of the Helmholtz equation with high wave number. Part I: The h-version of the FEM. Computers & Mathematics with Applications. **30** (9), 9-37 (1995). doi:10.1016/0898-1221(95)00144-N
17. Junger, M. C., Feit, D.: Sound, Structures and Their Interaction. 2nd ed., MIT Press, Cambridge, MA (1986)
18. Kress, R.: Linear Integral Equations. 3rd ed., Applied Mathematical Sciences, vol. 82, Springer, New York (2014). doi:10.1007/978-1-4614-9593-2
19. Kupradze, V. D., Aleksidze, M. A.: The method of functional equations for the approximate solution of certain boundary value problems. USSR Computational Mathematics and Mathematical Physics. **4** (4), 82-126 (1964). doi:10.1016/0041-5553(64)90006-0
20. Lavryk, S.: On the numerical solution of the three-dimensional Dirichlet problem for the Helmholtz equation in case of regions with smooth boundaries. Visnyk Lviv Univ. Ser. Appl. Math. Comp. Sci. **12**, 1-9 (2006)
21. Lin, J., Chen, C. S., Liu, C.-S.: Fast solution of three-dimensional modified Helmholtz equations by the method of fundamental solutions. Communications in Computational Physics. **20** (2), 512-533 (2016). doi:10.4208/cicp.060915.301215a
22. Lin, J., Chen, W., Wang, F.: A new investigation into regularization techniques for the method of fundamental solutions. Mathematics and Computers in Simulation. **81** (6), 1144-1152 (2011). doi:10.1016/j.matcom.2010.10.030
23. Marin, L.: A meshless method for the numerical solution of the Cauchy problem associated with three-dimensional Helmholtz-type equations. Applied Mathematics and Computation. **165** (2), 355-374 (2005). doi:10.1016/j.amc.2004.04.052
24. Wienert, L.: Die numerische Approximation von Randintegraloperatoren für die Helmholtzgleichung im $\mathbb{R}^3$. PhD thesis, University of Goettingen (1990)
25. Wu, T., Xu, R.: An optimal compact sixth-order finite difference scheme for the Helmholtz equation. Computers & Mathematics with Applications. **75** (7), 2520-2537 (2018). doi:10.1016/j.camwa.2017.12.023
26. Ushijima, T., Chiba, F.: Error estimates for a fundamental solution method applied to reduced wave problems in a domain exterior to a disc. Journal of Computational and Applied Mathematics. **159** (1), 137-148 (2003). doi:10.1016/S0377-0427(03)00559-4

Received 17.05.2025
Revised 10.06.2025